

# MULTI-OBJECTIVE EXTREMUM SEEKING TO CONTROL DRIFTS IN THE TRANSVERSE BEAM SPLITTING EFFICIENCY OF THE MULTI-TURN EXTRACTION AT THE CERN PROTON SYNCHROTRON

C. Uden\*, A. Huschauer, V. Kain, M. Schenk, N. Madysa, H. Pahl, CERN, Geneva, Switzerland

## Abstract

Time-varying pulse to pulse fluctuations of the intensity sharing between the islands and the core of the CERN Proton Synchrotron (PS) Multi-Turn Extraction (MTE) constitute a main source for manual adjustment of this beam type. The application of an online controller is explored to further enhance both operational autonomy of the accelerator and physics performance. In this contribution a proof of concept implementation of a multi-objective extremum seeking algorithm is presented. The tuning of the PS parameters, the proper choice of the hyperparameters of the algorithm and the achievements reached during the studies are summarised.

## INTRODUCTION

The beam for the Super Proton Synchrotron (SPS) fixed-target physics programme has been using the MTE scheme in the PS since 2015. Five beamlets, one central core and four surrounding islands, are created by adiabatically crossing a resonance excited by non-linear magnetic elements [1]. Amidst several successful improvements since its introduction [2], the mitigation of time-varying pulse to pulse performance fluctuations remains troublesome to this day.

The performance of the MTE scheme is quantified by the splitting efficiency  $\eta_{\text{MTE}}$  [3], which is defined as ratio of the average intensity per island over the total intensity. The nominal value of  $\eta_{\text{MTE}}^{\text{nominal}} = 0.2000$  corresponds to equal intensity sharing between the core and the islands.

The root-cause of the performance fluctuations are twofold and are summarised in two scenarios: marginal and stark changes in external conditions. Both scenarios are unavoidable in real world application and require case dependent solutions.

The effects of marginal changes on the evolution of  $\eta_{\text{MTE}}$  are subtle to observe. The hypothesis is that this is due to temperature fluctuations, which modify the magnetic properties. Figure 1 demonstrates a typical drifting trend. During this time period, an identical magnetic configuration of the PS was ensured and no settings were modified.

On the other hand, the performance of the MTE scheme is strongly influenced by stark changes in external conditions such as variations in magnetic properties at the beginning of the cycle. As the position of the islands in horizontal phase space is proportional to the horizontal betatron tune of the PS, stark magnetic changes result in a step variation in the evolution of  $\eta_{\text{MTE}}$ , which is clearly identified in specific patterns of preceding magnetic configurations of the machine.

\* Also at Karlsruhe University of Applied Sciences, DE-76012 Karlsruhe

To stabilise the drifting trends of  $\eta_{\text{MTE}}$ , the operators of the PS have to intervene manually on a regular basis in order to counteract the performance fluctuations induced by the marginal and stark changes in external conditions. As changes of the magnetic history in the PS are common due to the cycling nature of the machine, the primary setting to steer against the fluctuation is the horizontal tune. Additionally, a horizontal excitation (HE) is applied during the MTE process to help equalise the intensity population between the islands and the core. The frequency and amplitude of the HE are parameters to control the splitting efficiency as well as the flatness of the extracted five-turn long spill.

Amidst all efforts of manual adjustments, which had to be performed on average 1.6 times a day during the 2022 physics run, the median value of  $\eta_{\text{MTE}}$  reached 0.19791 with a standard deviation of  $\sigma = 0.00510$ . While the performance is acceptable, the goal of the presented studies has been to enhance the performance while simultaneously increasing the degree of autonomy to perform this task. The distribution of all relevant cycles during the 2022 physics run is shown in Fig. 2.

To mitigate the performance fluctuations and specifically to counteract the recurring drifts, the implementation of an Extremum Seeking (ES) algorithm to act as an online control and optimisation loop following [4] was explored and results are presented in this contribution.

## ES FRAMEWORK

### Loss-function design

The primary design objective is to keep  $\eta_{\text{MTE}}$  as close as possible to its nominal value. Due to a strong correlation between beam quality for the downstream experiments and tiny fluctuations in  $\eta_{\text{MTE}}$ , notable on a scale of  $5 \times 10^{-3}$ , com-

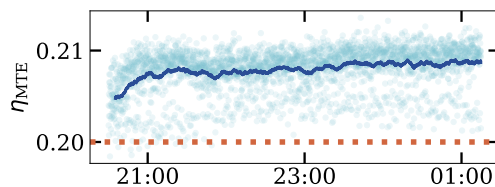


Figure 1: Demonstration of drifts in transverse beam splitting efficiency induced by marginal changes in external conditions. The red dotted line represents  $\eta_{\text{MTE}}^{\text{nominal}}$ . The cloud of raw data points during this time-series is shown in the background of the plot while the thick blue line shows the rolling mean indicating the trend of the evolution.

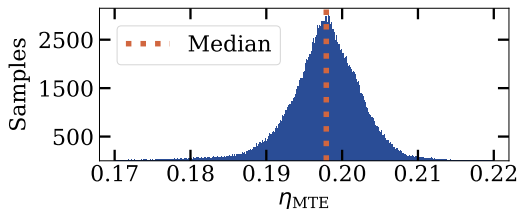


Figure 2: Distribution of  $\eta_{\text{MTE}}$  for all relevant 2022 operational cycles for the SPS fixed-target programme physics production. The samples were cleared of outliers, only considering cycles of the operational cycle with a fixed configuration of preceding magnetic properties and only containing cycles that were successfully delivered to the SPS. Sample size: 282k.

mon loss-functions such as the mean squared error (MSE) result in vanishing rewards near the optimum. To address this issue, a logarithmic objective was adopted, following the research results presented in [5].

This observation resulted in a tailored loss-function defined as follows:

$$C_{\eta}(\eta_{\text{MTE}}) = \ln(1 + \alpha_{\eta} |\eta_{\text{MTE}} - \eta_{\text{MTE}}^{\text{nominal}}|), \quad (1)$$

where  $\alpha_{\eta} = 5000$  is a factor to control the steepness of the convergence towards  $\eta_{\text{MTE}}^{\text{nominal}}$ . The behaviour of  $C_{\eta}$  as a function of  $\eta_{\text{MTE}}$  is shown in Fig. 3.

While  $\eta_{\text{MTE}}$  is the primary figure of merit for the quantification of the MTE process, the setting of the HE has to be taken into account. Increasing the amplitude of the HE typically improves the efficiency of the transverse splitting process, with the major drawback of simultaneously increasing the transverse beam emittance. This physical effect has to be taken into account to prevent the algorithm from relentlessly increasing the HE amplitude.

To prevent this side-effect,  $C_{\text{HE}}$  was designed as an additional auxiliary loss-function which will be added to  $C_{\eta}$  in order to constrain  $s_{\text{amp}}$ :

$$C_{\text{HE}}(s_{\text{amp}}, s_{\text{opt}}) = e^{(\alpha_{\text{amp}}(s_{\text{amp}} - s_{\text{opt}}))}, \quad (2)$$

where  $s_{\text{amp}}$  is the current setting of the HE amplitude and  $s_{\text{opt}}$  is its optimal setting.  $\alpha_{\text{amp}} = 16$  is a factor to control the start of the exponential growth of the slope beyond  $s_{\text{opt}}$ . The design idea is that  $w_{\text{HE}} \leq 1$  whenever  $s_{\text{amp}} \leq s_{\text{opt}}$  and that

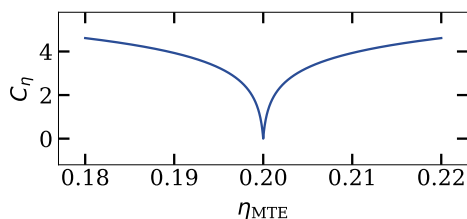


Figure 3: Resulting cost of  $C_{\eta}$  as a function of  $\eta_{\text{MTE}}$ .

$w_{\text{HE}}$  increases exponentially within the interval of relevant values of  $s_{\text{amp}}$ . Figure 4 visualises these properties and shows the interval of realistic values of  $s_{\text{amp}}$  on the x-axis.

The resulting loss-function is defined as

$$C(\eta_{\text{MTE}}, s_{\text{amp}}, s_{\text{opt}}) = C_{\eta}(\eta_{\text{MTE}}) + C_{\text{HE}}(s_{\text{amp}}, s_{\text{opt}}) \quad (3)$$

### Action Space

Equation (3) was implemented and used with the recently published version of the *CERNML Extremum Seeking* [6] framework. Different values of hyperparameters were explored and the default values as configured in the referenced version have been found out to work best for controlling the MTE splitting [7].

For the ES controller to interact with the PS, its action space is described by a dedicated actuator of the parameters “horizontal tune”, “HE frequency” and “HE amplitude”. The parameter values are restricted to symmetric intervals around their initial values quantified by  $\Delta_{\text{tune}}$ ,  $\Delta_{\text{freq}}$  and  $\Delta_{\text{amp}}$ , respectively. These intervals are linearly mapped to the action interval  $[-1; 1]$  based on  $\pm\Delta_{\{\text{tune}, \text{freq}, \text{amp}\}}$ .

Following thorough hyperparameter tuning, the values  $\Delta_{\text{tune}} = 15 \times 10^{-4}$ ,  $\Delta_{\text{freq}} = 6 \times 10^{-5}$  and  $\Delta_{\text{amp}} = 0.08$  were chosen for the subsequent experiments.

## EXPERIMENTAL RESULTS

Figure 5 shows the evolution of  $\eta_{\text{MTE}}$  with and without the active control algorithm and demonstrates the effectiveness of ES to counteract the performance drift.

Figure 6 summarises the distribution of  $\eta_{\text{MTE}}$  over the entirety of the experimental campaign. Its median value of 0.20008 and standard deviation  $\sigma = 0.00328$  substantiates the outstanding performance of ES compared to the manually adjusted operational results shown in Fig. 2.

### Observations

ES requires that the system it operates upon is reinitialised repeatedly with the same initial conditions [4]. Figure 7 shows an actuator behaving as expected in a validated environment without any stark changes in external conditions. However, it was observed that specific configurations of preceding magnetic properties of the machine caused the algorithm to malfunction. Figure 8 is an example of what

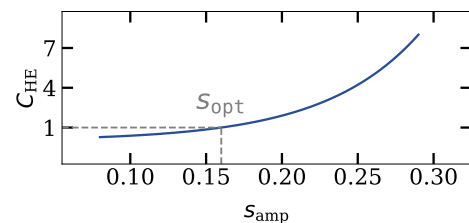


Figure 4: Result of  $w_{\text{HE}}$  as a function of the setting of the HE amplitude. For this example,  $s_{\text{opt}} = 0.16$  and is visualised by the grey dashed line.

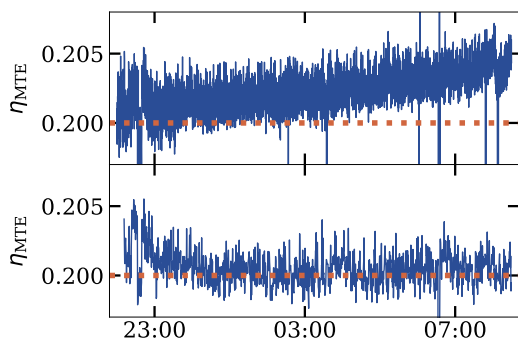


Figure 5: Comparison of the evolution of  $\eta_{MTE}$  for the operational (upper) and experimental (lower) cycles. A clear drift with a trend to move away from  $\eta_{MTE}^{nominal}$  is visible for the operational cycles. It was made sure that no settings were modified during this time frame. The lower plot shows the results when controlling the performance by ES. Both cycles were executed in a specific sequence during the same time period in order for the operational cycle to act as a control group.

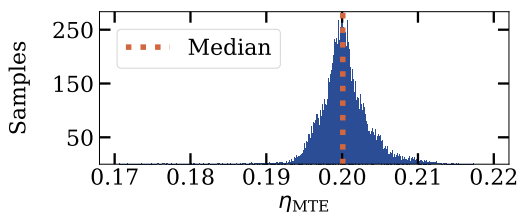


Figure 6: Distribution of  $\eta_{MTE}$  for all relevant experimental cycles. The samples were cleared of outliers and only consider cycles in a validated environment of external conditions that are known to respect the functional requirements of ES. Sample size: 14.8k.

can happen when the system is reinitialised with different initial conditions.

Mitigation strategies for such cases are currently being studied. Within such a dynamic environment present at a cycling machine like the PS, imposing even stricter restrictions on the configuration of preceding cycles and their impact on magnetic properties is not feasible.

## CONCLUSION AND OUTLOOK

ES was successfully tested at the PS to control the MTE splitting and mitigate its dependency on external perturbations.

Following the successful experimental campaign, efforts are currently ongoing to validate the effectiveness of the current ES implementation in the presence of longitudinal barrier buckets [8] as the changes require  $\eta_{MTE}$  to be redefined.

Additionally, the spill flatness, another aspect of spill quality, is currently disregarded by the implementation of

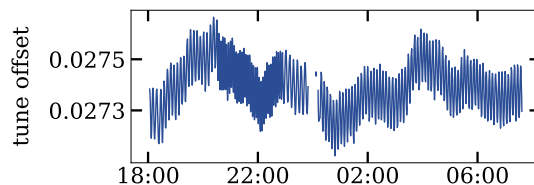


Figure 7: Demonstration of the "tune" actuator which modifies the tune offset, controlled by ES, in a validated external environment. The evolution is characterised by sinusoidal waves.

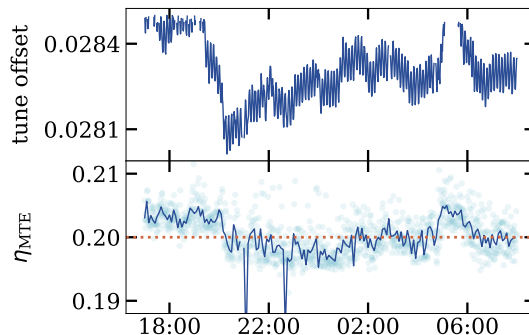


Figure 8: Example of the evolution of the tune offset in violated external conditions. Abrupt changes in its trend which break the sinusoidal oscillation (upper) were frequently observed when the evolution of  $\eta_{MTE}$  (lower) showed a step variation, the data shown has been re-sampled over non-overlapping 8 minute intervals.

ES due to a lack of an adequate observable. A new metric following the concepts described by the parameter  $\lambda_{eff}^n$  in [9] is currently being developed.

ES is currently ran in a graphical user interface to facilitate the experimental process. An operational implementation requires the framework to run on a server, which is planned to be available early summer 2023.

## ACKNOWLEDGEMENTS

Our warm thanks go to the PS Operations crew for the ongoing support during the extensive testing campaign.

## REFERENCES

- [1] A. Huschauer, H. Bartosik, S. Cave, M. Coly, D. Cotte, H. Damerau, G. P. Giovanni, S. Gilardoni, M. Giovannozzi, V. Kain, E. Koukovini-Platia, B. Mikulec, G. Sterbini and F. Tecker, "Advancing the CERN proton synchrotron multi-turn extraction towards the high-intensity proton beams frontier", in *Physical Review Accelerators and Beams*, **22**, 2019. doi:10.1103/PhysRevAccelBeams.22.104002
- [2] A. Huschauer, M. Giovannozzi, O. Michels, A. Nicoletti and G. Sterbini, "Analysis of Performance Fluctuations for the CERN Proton Synchrotron Multi-Turn Extraction" in *J. Phys.: Conf.*

- Ser.*, **874**, 012072, 2017. doi:10.1088/1742-6596/874/1/012072
- [3] A. Huschauer, A. Blas, J. Borburgh, S. Damjanovic, S. Gilardoni, M. Giovannozzi, M. Hourican, K. Kahle, G. Le Godec, O. Michels, G. Sterbini and C. Hernalsteens, “Transverse beam splitting made operational: Key features of the multiturn extraction at the CERN Proton Synchrotron” in *Phys. Rev. Accel. Beams*, **20**, 061001, 2017. doi:10.1103/PhysRevAccelBeams.20.061001
- [4] A. Scheinker and D. Scheinker, “Extremum seeking for optimal control problems with unknown time-varying systems and unknown objective functions”, in *Int. J. Adapt. Control Signal Process.*, **35**, 7, 1143–1161, 2021. doi:10.1002/acs.3097
- [5] J. Kaiser, O. Stein and A. Eichler, “Learning-based Optimization of Particle Accelerators Under Partial Observability Without Real-World Training”, in *Proceedings of the 39th International Conference on Machine Learning*, 2022. doi:162:10575–10585
- [6] N. Madysa, “CERNML Extremum Seeking”, CERN, v2.0.0, 20. Jul. 2022. <https://gitlab.cern.ch/geoff/optimizers/cernml-extremum-seeking/-/tags/v2.0.0>
- [7] N. Madysa, “CERNML Extremum Seeking”, CERN, v2.0.0, 20. Jul. 2022. [https://gitlab.cern.ch/geoff/optimizers/cernml-extremum-seeking/-/blob/v2.0.0/src/cernml/extremum\\_seeking/\\_\\_init\\_\\_.py#L272](https://gitlab.cern.ch/geoff/optimizers/cernml-extremum-seeking/-/blob/v2.0.0/src/cernml/extremum_seeking/__init__.py#L272)
- [8] M. Vadai, A. Alomainy, H. Damerau, S. Gilardoni, M. Giovannozzi and A. Huschauer, “Beam manipulations with barrier buckets in the CERN PS”, 2019. doi:10.18429/JACoW-IPAC2019-MOPTS107
- [9] M. Pari, “Study and development of SPS slow extraction schemes and focusing of secondary particles for the ENU-BET monitored neutrino beam”, Ph.D. thesis, Universita’ degli Studi di Padova, Padova. Italy, 2020.